# CHAPTER V
# NON ISOTHERMAL CRYSTALLIZATION KINETICS AND MELTING BEHAVIORS OF THERMOPLASTIC/LIQUID CRYSTALLINE POLYMER BLENDS OF POLY(TRIMETHYLENE TEREPHTHALATE)/VECTRA A950

## 5.1 Abstract

The non-isothermal crystallization and subsequent melting behaviors of poly(trimethylene terephthalate), (PTT)/Vectra A950, (VA) blends with different VA contents were studied by differential scanning calorimetry. The effects of VA on the non-isothermal crystallization kinetics of PTT were discussed based on the Ozawa model. It was found that VA has a nucleation effect on PTT crystallization. The triple melting endotherms were found in the subsequent melting thermograms. The blends are clearly immiscible as verified by the unchanged $T_g$ and morphological results.

**Key words:** Blends; Non-Isothermal Crystallization Kinetics; Liquid Crystalline Polymer; Poly(trimethylene terephthalate)

## 5.2 Introduction

To obtain the engineering performance of polymers, fiber-reinforced composites have been made for industrial products for many years. However, those fibrous fillers can have many drawbacks like causing abrasion on processing machines, and a rise in melt viscosity. Blending a thermoplastic (TP) with a thermotropic liquid crystalline polymer (LCP) has become an interesting choice because of the possible enhanced processibility and improved mechanical properties; i.e. under proper flow conditions, the LCP domains can align themselves and elongate to the direction of flow causing a reduction in melt viscosity as well as reinforcing effects. Therefore, these

blends have been termed 'in-situ composites'. Another factor that influences the physical properties is the extent of crystallization occurring during processing. However, there have been contradictory results regarding the effects of Vectra A950 (VA), a liquid crystalline polymer, on the crystallization kinetics of poly(ethylene terephthalate) (PET). For example, VA was found to act as a nucleating agent upon PET crystallization [1, 2] while Magagnini and coworkers [3] observed the retardation of the dynamic crystallization of PET by VA. The contradictory results obtained so far indicated the necessity for further investigation on the crystallization kinetics of binary blends of VA with other terephthalate-based polyesters, like poly(trimethylene terpthalate) (PTT).

In this contibution, studies on VA/PTT blends under non-isothermal conditions were conducted by differential scanning calorimetry (DSC). The effects of VA on the crystallization kinetics of PTT were analyzed based on the Ozawa equation. The subsequent melting endotherms were also investigated. The morphology of the blends with 10 wt% VA was studied by scanning electron microscopy (SEM).

## 5.3 Experimental

### 5.3.1 Materials

Poly(trimethylene terephthalate) (PTT) was kindly supplied by PTT PolyCanada LP (Corterra 9200). Its intrinsic viscosity (IV) is 0.92 dl/g. The LCP used was Vectra A950 (labeled VA hereafter) was supplied by Hoechst-Celanese. VA is a copolyester of 73 mol % phydroxybenzoic acid (HBA) and 27 mol % 2-hydroxy-6-naphthoic acid (HNA). The viscosity of the neat PTT and the neat VA as determined in our laboratory using a CEAST Rheologic 5000 twin-bore capillary rheometer at 280°C, shear rate of 2000 $s^{-1}$ and a capillary die with a length-to-diameter ratio of 20, are 5.15 and 47.59 Pa.s respectively. The materials were dried in a vacuum oven at 130°C for at least 12 h prior to use.

5.3.2 Preparation of Blends

PTT and VA resins were premixed in a dry mixer to prepare PTT/VA blends with VA contents of 0, 10, 30, and 70 wt% respectively. The samples were designated as follows: VA wt %. For example, a blend containing 10 wt% VA and 90 wt% PTT would be named VA10. The dry-mixed blends were melt-mixed in a self-wiping, co-rotating twin-screw extruder (Collin, ZX-25). The temperature of the barrel section from the feeding zone to the die was set at 80, 230, 250, 275, 285, and 265°C. The rotor was operated at a speed of 30 rpm. The extrudates were cooled by water and then pelletized.

5.3.3 Differential Scanning Calorimetry (DSC) Procedures

The The non-isothermal crystallization behavior of the neat PTT, Vectra and their blends was analyzed using a Mettler-Toledo DSC822$^e$ differential scanning calorimeter (DSC). The temperature scale of the DSC was calibrated from the melting point (156.60°C) of high purity (99.999%) indium metal. The power response of the calorimeter was calibrated from the enthalpy of fusion of indium, taken to be 28.45 J/g. To avoid an uneven thermal conduction of the samples, each sample holder was loaded with sample of comparable quantity (6±0.5 mg). All DSC analyses were performed under dry nitrogen atmosphere. Each sample was heated from 25°C at a heating rate of 80°C/min to a fixed melt-annealing temperature of 310°C for 5 min in order to ensure complete melting. Then, each sample was cooled at a cooling rate ranging from 10 to 25°C/min, to 120°C. The non-isothermal melt crystallization exotherms, the peak crystallization temperature $T_{cp}$, the half-time of crystallization ($t_{0.5}$), and the heat of crystallization $\Delta H_c$ were recorded. $\Delta H_c$ values were then normalized by the weight percent of a certain component to yield $\Delta H^*_c$. After the cooling process, each sample was then heated to 300°C at a rate of 10°C/min to obtain the subsequent melting endotherms. To obtain the glass transition temperature, a seperate experiment was done; after erasing the thermal history of the sample, the sample was then quenched in liquid nitrogen to

achieve the completely amorphous state of the samples. The quenched sample was immediately subjected to a heating scan at a rate of 5°C/min from 25°C to 300°C.

5.3.4 Morphological Observation

VA10 samples obtained from a twin-screw extruder and a capillary rheometer were immersed in 1,2-dichlorophenol at 80°C for 2 h to dissolve the PTT matrix as the first step, followed by repeated washing of the residue for a clear VA phase. The LCP residue was then sputtered with a thin layer of gold prior to observation. The morphological observation was performed using a JEOL JSM5200 scanning electron microscope (SEM) operated at 15 kV.

## 5.4 Results and Discussion

Fig. 5.1 displays the non-isothermal melt crystallization exotherms for VA10 at a cooling rate ranging from 10 to 25°C/min. The displayed exothermic peaks are ascribed to the melt crystallization peaks of PTT [4]. The VA peaks were too weak to be displayed properly, so they were excluded, and only the data belonging to the PTT phase were tabulated here (see Table 5.1). The $T_{cp}$ values shift to lower temperature with increasing cooling rate, as expected. The greater $T_{cp}$ infers a faster initiation of the melt crystallization process. At a fixed cooling rate, the initiation rate of crystallization follows the order: VA30 > VA10 > VA70 > PTT. The half-time of crystallization ($t_{0\,5(l)}$), defined as the time required to attain half of the final crystallinity, is mostly ranked as follows: PTT > VA70 > VA30 > VA10. Therefore, the presence of VA can enhance the melt crystallization process of PTT. However, at a very high VA content like VA70, the rate of the melt crystallization process of PTT is lower than VA10 and VA30 due to the dilution of PTT concentration upon blending with VA. The normalized crystallization enthalpy can be used to determine the crystallization extent during melt crystallization; that is, the larger the $\Delta H^*_c$, the greater the crystallization extent. At every cooling rate, $\Delta H^*_c$ is in the following order: VA10 > VA30 > PTT > VA70. This arises from the fact

that the addition of VA can increase the crystallization temperature, which results in a longer crystallization time and an increase in the rate of crystallization, as reflected in the values of $t_{0.5(l)}$. Thus VA10 and VA30 exhibit higher $\Delta H^*_c$ values than PTT and VA70. However, Sharma *et al.* [1] has claimed that the excessive nucleation at the interface with the matrix may lead to an imperfect crystal formation, thus lowering the extent of crystallization. This should be the case of the lowest crystallization extent of VA70.

For a long time, the non-isothermal crystallization of polymers has been investigated by many researchers, as semicrystalline polymers are commonly processed under non-isothermal conditions. Although the process of non-isothermal crystallization of slowly crystallizing materials, like polymers, is relatively complex, it is very attractive to describe it using rather simple models. One of the methods commonly applied for the analysis of non-isothermal crystallization kinetic data was proposed by Ozawa [5, 6] who extended the Avrami equation [7, 8], which is applicable to the isothermal system, to fit the non-isothermal case by assuming that the sample was cooled with a constant rate from the molten state.

The Ozawa equation is expressed as follows:

$$1 - C(T) = \exp\left[-\frac{K(T)}{\phi_m}\right], \tag{5.1}$$

where C(T) is the relative degree of crystallinity at temperature T, K(T) is the crystallization rate constant, φ is the cooling rate, and m is the Ozawa exponent relating to the mechanism of nucleation and dimension of crystal growth. The double-logarithmic form of Eq. (5.1) is:

$$\ln[-\ln(1/C(T)] = \ln K(T) - m\ln\phi \tag{5.2}$$

If a linear relationship is achieved when $\ln[-\ln(1/C(T)]$ is plotted against $\ln\phi$, the Ozawa equation is then satisfactory in describing the non-isothermal crystallization process of that particular system. The Ozawa rate constant, $K(T)$, could be calculated from the anti-natural logarithmic value of the y-intercept, and the Ozawa exponent $m$ is the slope. The values of $m$ and $K(T)$ for each sample are listed in Table

5.2. It was found that the Ozawa rate constants of all the sample types studied are in the following order: VA10 > VA30 > VA70 > PTT.

Fig. 5.3 shows the subsequent melting endotherms of the neat PTT and PTT/VA blends at 10, 30, and 70 wt% VA after non-isothermal melt-crystallization at a cooling rate of 15°C/min. Clearly, triple melting endotherms were observed. These endotherms were labeled as peaks I, II, and III for low-, middle-, and high-temperature melting endotherms, respectively. Peak I was found to correspond to the melting of the primary crystallites formed at the crystallization temperature and peaks II and III correspond to the melting of recrystallized crystallites of different stabilities formed during a heating scan [9]. As depicted in Fig. 5.3, with increasing VA content, peak I shifted to higher temperature, indicating that VA could increase the thermal stability of the PTT crystalline phase. Because of the small fraction of PTT in VA70, we could not obtain its glass transition temperature ($T_g$) and only the $T_g$ values of PTT, VA10, and VA30 are plotted in Fig. 5.4 (all are approximately 42°C). In our experiments, VA10 and VA30 are immiscible, as indicated by a single composition-independent $T_g$ belonging to the PTT phase. This is not surprising since VA molecules are rigid while PTT molecules are flexible and coil-like [10]. The smooth surfaces of VA domains extracted from the VA10 samples clearly depict its immiscibility (see Fig. 5.5a-b). As shown in Fig. 5.5(b), the elongated VA domains observed in VA10 after extrusion through a capillary die indicate the influence of processing conditions on the final phase morphology of the blends and also indicate the potential of VA as a reinforcing agent in the PTT matrix.

## 5.5 Conclusions

The non-isothermal crystallization behaviors, subsequent melting behaviors, and the phase morphology of poly(trimethylene terephthalate) (PTT)/Vectra A950 (VA) blends were studied. The presence of VA could enhance the crystallization rate of the PTT fraction in the blends according to the Ozawa approach. This increase in the

crystallization rate is ascribed to the nucleation effect of VA. Also, VA gives rise to a higher normalized crystallization extent in blends with 10 and 30 wt% VA. Triple melting endotherms were obtained. The incorporation of VA also enhances the thermal stability of the PTT primary crystallites. The glass transition temperatures were found to be constant regardless of the VA content. The morphology and the unchanged glass transition temperature signified the immiscibility of the PTT/VA blends. .

## 5.6 Acknowledgements

The authors are grateful for the financial support of the Royal Golden Jubilee Ph.D. Program.

## 5.7 References

[1] Sharma SK, Tendolkar A, Misra A. Mol Cryst Liq Cryst 1988;157:597-614.

[2] Melot D, MacKnight WJ. Polym Adv Technol 1992;3:383-388.

[3] Magagnini PL, Tonti MS, Masseti M, Paci M, Minkova LI, Miteva TT. Polym Eng Sci 1998;38:1572-1586.

[4] Dangseeyun N, Supaphol P, Nithitanakul M. Polym Test 2004;23:187-194.

[5] Ozawa T. Polymer 1971;12:150-158.

[6] Jeziorny A. Polymer 1978;19:1142-1144.

[7] Avrami M. J Chem Phys 1936;7:1103-1112.

[8] Avrami M. J Chem Phys 1940;8:212-224.

[9] Chen X, Hou G, Chen Y, Yang K, Dong Y, Zhou H. Polym Test 2007;26:144-153.

[10] Flory PJ. Macromolecules 1978;11:1138-1141.

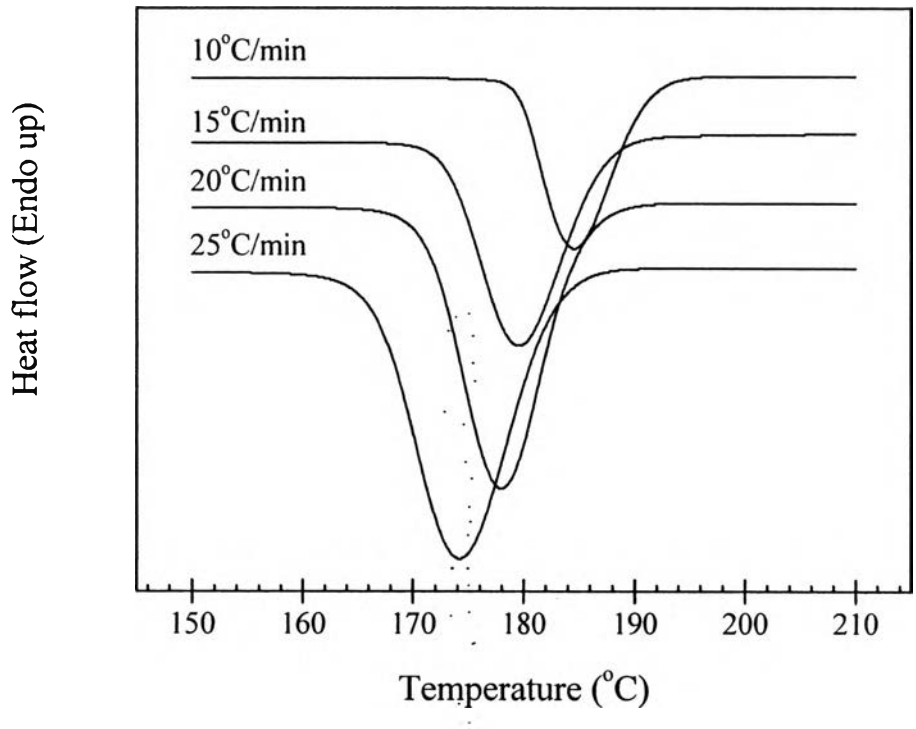


**Figure 5.1** Non-isothermal melt crystallization exotherms for VA10 at various cooling rates.

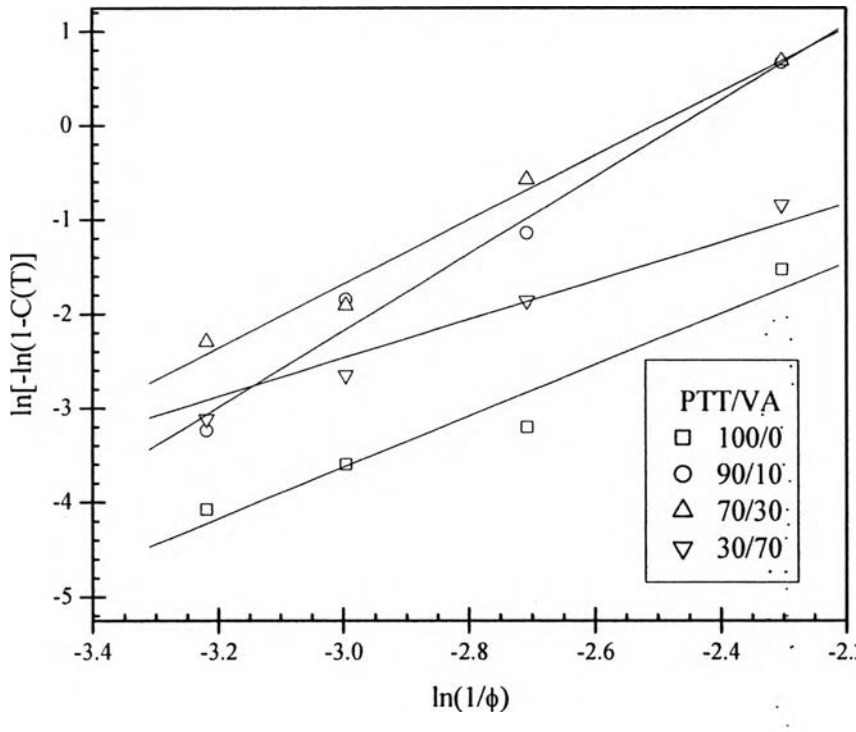


**Figure 5.2** Plots of $\ln\phi$ versus ln t for the neat PTT at various relative crystallinities.

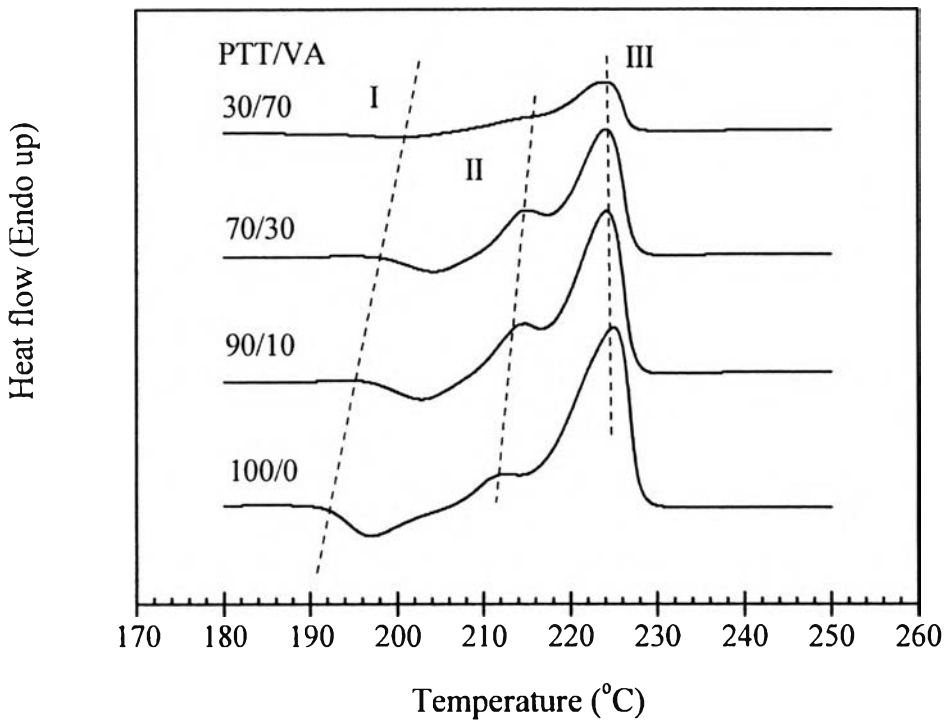


**Figure 5.3** Subsequent melting endotherms of the neat PTT and PTT/VA blends at 10, 30, and 70 wt% VA after non-isothermal melt-crystallization at a cooling rate of 15°C/min.

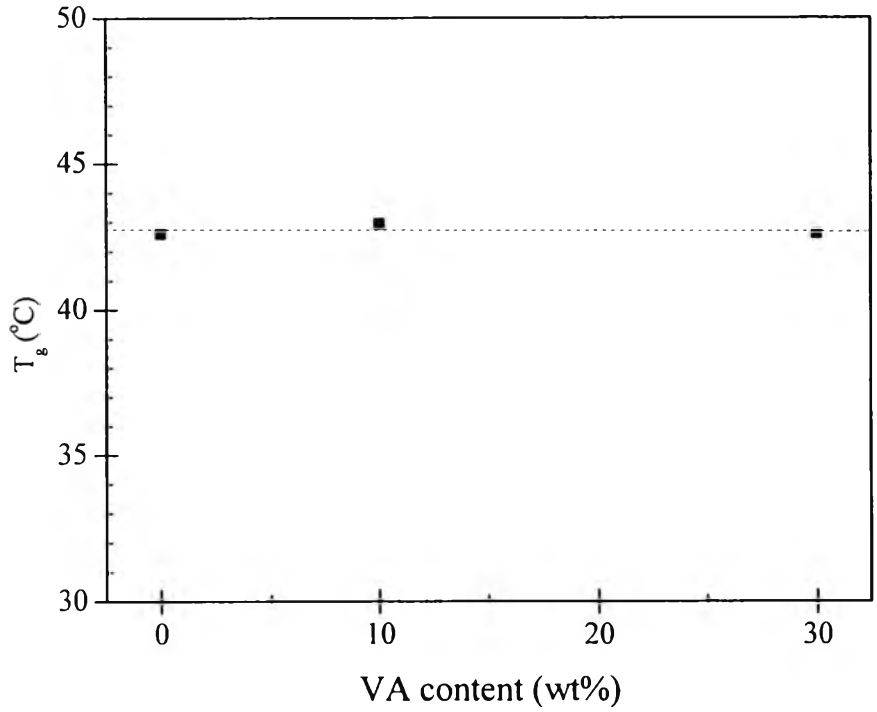


**Figure 5.4** Glass transition temperature ($T_g$) for the neat PTT and its blend with 10 and 30 wt% VA.

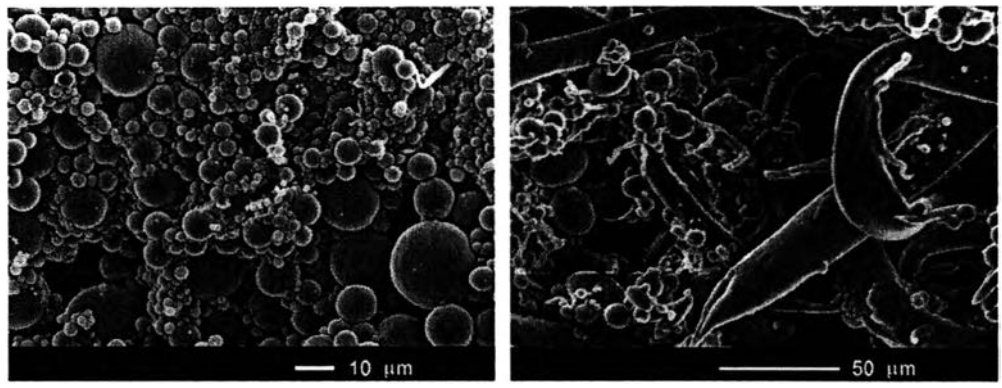


**Figure 5.5** Scanning electron micrographs of VA residues of VA10 extrudates from a twin-screw extruder (left) and a capillary rheometer (right).

**Table 5.1** Characteristic data of non-isothermal melt-crystallization exotherms for the neat PTT and PTT/VA blends at various cooling rates

| Cooling rate [°C/min] | Sampl | $T_{cp(I)}$[°C] | $\Delta H_{c(I)}$ [J/g] | $\Delta H^{*}_{c(I)}$ [J/g][a] | $t_{0.5(I)}$ [s] |
|---|---|---|---|---|---|
| 10 | PTT | 177.2 | 60.20 | 60.20 | 70.8 |
| | VA10 | 184.9 | 59.96 | 66.62 | 39.6 |
| | VA30 | 186.0 | 45.76 | 65.37 | 36.6 |
| | VA70 | 180.8 | 13.61 | 45.37 | 58.8 |
| 15 | PTT | 170.6 | 61.00 | 61.00 | 58.2 |
| | VA10 | 180.0 | 58.60 | 65.10 | 30.6 |
| | VA30 | 181.3 | 44.60 | 63.70 | 30.6 |
| | VA70 | 176.9 | 13.90 | 46.30 | 42.0 |
| 20 | PTT | 168.4 | 57.27 | 57.27 | 46.8 |
| | VA10 | 178.0 | 58.56 | 65.07 | 22.8 |
| | VA30 | 179.6 | 43.68 | 62.40 | 28.8 |
| | VA70 | 173.2 | 10.41 | 34.70 | 33.0 |
| 25 | PTT | 165.1 | 60.40 | 60.40 | 39.0 |
| | VA10 | 174.8 | 54.87 | 60.97 | 20.4 |
| | VA30 | 176.5 | 42.42 | 60.60 | 23.4 |
| | VA70 | 174.5 | 12.19 | 40.63 | 31.8 |

**Table 5.2** Non-isothermal crystallization kinetic parameters based on the Ozawa method at a temperature of 182°C and cooling rates ranging from 10 to 25°C/min

| Sample | m | K (°C/min) |
|---|---|---|
| PTT | 2.72 | $9.24 \times 10^{1}$ |
| VA10 | 4.06 | $2.24 \times 10^{4}$ |
| VA30 | 3.40 | $5.02 \times 10^{3}$ |
| VA70 | 2.04 | $1.39 \times 10^{2}$ |